

On the Low Temperature and Low Pressure Regime Diagram of n-Heptane Droplet Burning in Microgravity

Wenyi Zhang, Yu Cheng Liu

Center for Combustion Energy, Tsinghua University, Beijing 100084, China

Department of Energy and Power Engineering, Tsinghua University, Beijing 100084, China

Key Laboratory for Thermal Science and Power Engineering of Ministry of Education, Tsinghua University, Beijing 100084, China

1 Abstract

The present study investigates the n-heptane droplet burning with ambient conditions 600-1000 K and 0.1 - 2 bar through numerical simulations. Experimental data (initial droplet size 0.7 mm, pressure down to 1 bar) from microgravity experiments offer validation of our 1-D modeling for characteristic time scales identified throughout the droplet lifetime. The motivation of this study is the seemingly narrowing cool flame regime towards the low-pressure conditions presented by prior experimental and numerical works, as contrast to the diverging negative temperature coefficient region for lower pressures. Results for sub-atmospheric pressure show that the cool flame area on the regime diagram converges with decreasing pressure due to major contribution from the ceiling temperature effect. Moreover, the physics trigger at various chemical time scales are well bounded by the droplet lifetime such that very long ignition delay becomes irrelevant to droplet problems.

Keywords: n-heptane, droplet cool flame, microgravity, numerical simulation

2 Introduction

Owing to the realistic demand of high energy density and less requirements for storage for general fuels, hydrocarbon liquid fuels have been the most common energy sources for transportation. Achieving more efficient utilization and low emission of such a liquid phase fuel have led to several areas of fundamental research including hydrocarbon oxidation kinetics and liquid combustion [1].

For liquid fuel combustion problems, droplets, sprays, or their combustion behavior in engines are among the most attractive yet difficult problems in the area due to interaction of multi-phase and complex physical and chemical processes. While the development of the D^2 law has brought insights to the sub-grid model in

a spray problem [2]. Its unique premise of spherical symmetry for a multi-phase combustion problem had further initiated the study of droplet burning with purposely minimized buoyancy convection, i.e. achieved by microgravity. In recent decades, experiments and detailed modeling for droplet burning in a microgravity environment have demonstrated that such an idealized problem, with validation from experimental data, offers advances towards better understanding of fundamental physics and more reasonable models in the spray sub-grid.

During the Flame Extinguishment (FLEX) Experiment in 2009 [3-4] onboard the International Space Station (ISS), the “cool flame” phenomena governed by low temperature fuel oxidation pathways at (600-800 K) were observed after the radiative extinction of a large droplet. Other ground-based experimental observations also suggest that when droplets are vaporizing at such a “low temperature” environment, the rate of droplet fuel consumption may well be affected by the low temperature oxidation chemistry [5]. More interestingly, for a given droplet size, a specific pressure to temperature regime diagram can be constructed to show the consequences of competition between high temperature and low temperature chemistry as well as droplet transport physics. Various distinct ignition categories can be found in such a diagram- single ignition (s.i), two-stage ignition (2 s.i.), cool flames, and no ignition (n.i.) as shown in Fig. 1.1a [6].

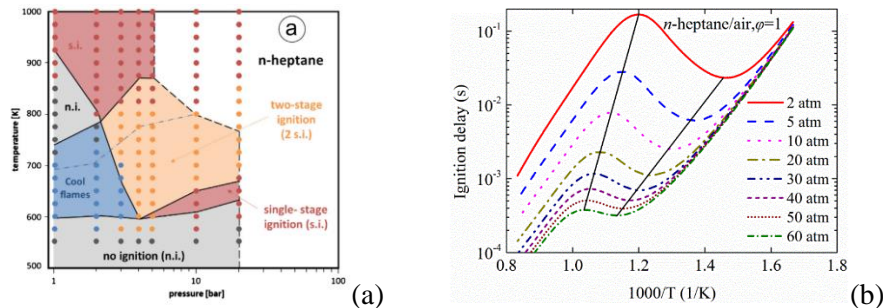


Figure 1.1 (a) Regime diagram for droplet ignition at various temperature and pressure (adapted from Cuoci et al. (2015) [6]); (b) pressure dependent effect on the ignition delay (adapted from Ji. et al. (2016) [7])

As suggested by Fig. 1.1a, decreasing pressure would lead to a narrower temperature region for cool flame. In contrast, the negative temperature coefficient region seems to become wider for lower pressures (see Fig. 1.1b). This discrepancy from a purely chemical description and multi-phase chemical-transport coupled phenomena roots the motivation of our study. In the present study, the pressure range is based on the availability of some experimental data [5] and extension to some special cases such as a flight cruising at a very high altitude, which requires reliable combustion at 0.5 bar and even lower [8]. The simulation results verified by the experimental data provided the details during the ignition and the steady burning processes, which provides confidence for the cases of extension towards the lower pressure.

3 Numerical methods

The numerical simulation in this work based on a 0.7 mm droplet suddenly exposed to a furnace environment with well-controlled pressure (1-2 bar) and temperature (600-1000 K) under microgravity, as described by Tanabe et al. [5]. The low pressure ambient of 0.1 to 1 bar are also considered.

In our spherically symmetric, 1-D, two-phase, constant pressure modeling, gas phase products do not penetrate across the interface; effects of supporting fiber, radiation, Dufour and Soret are found negligible.

The finite volume method (FVM) with first order time implicit is implemented on solving other terms. A staggered grid system is used to reduce oscillation as suggested by a typical FVM setup. This work adopts

40 uniform cells in the liquid phase, 200 non-uniform cells in the gas phases. The cell number remains the same in the process of simulation. Due to migration of the droplet surface after each time step, the cell locations are re-determined to accommodate the liquid-vapor boundary.

In this work, transient accumulation term, volumetric flux term, convection term, conduction term and chemical source term were considered in the energy equation and the species equation. The outer border is 200 times of initial droplet radius, and set as Dirichlet boundary, of which the initial conditions are identical to that of the gas phase. At the inner center of the droplet, no flux conditions are applied. At the droplet surface, the heat and mass conservations are described as Farouk et al. [9]. The Strang splitting method [10] is implemented on the solving algorithm so that the chemical source terms and other items of each time step are numerically decoupled. Based on the estimated diffusion time scale (i.e. 10^{-4} s), the solution time step of 10^{-5} s is adopted. Relative and absolute tolerance for temperature and all species mass fractions range from 10^{-5} to 10^{-6} .

An 88 species/387 reactions chemical kinetic model for n-heptane oxidation is used in this study [11]. This kinetic model was reduced from Mehl et al. [12] and hence include the low temperature kinetics for n-heptane oxidation.

4 Results and discussions

Figure 4.1 shows the comparison of simulation results and experimental data [5]. The definitions of the first induction time, total induction time and droplet life time are same as Cuoci et al. [6]. The simulation results have the same tendency as experimental data. This suggests that the model captures the most important physics of the problem. However, the values from the simulation are slightly lower than those from the experimental data. This difference could potentially stem from the chemical kinetic model as it may need further validation for ignition delay time under 3 bar.

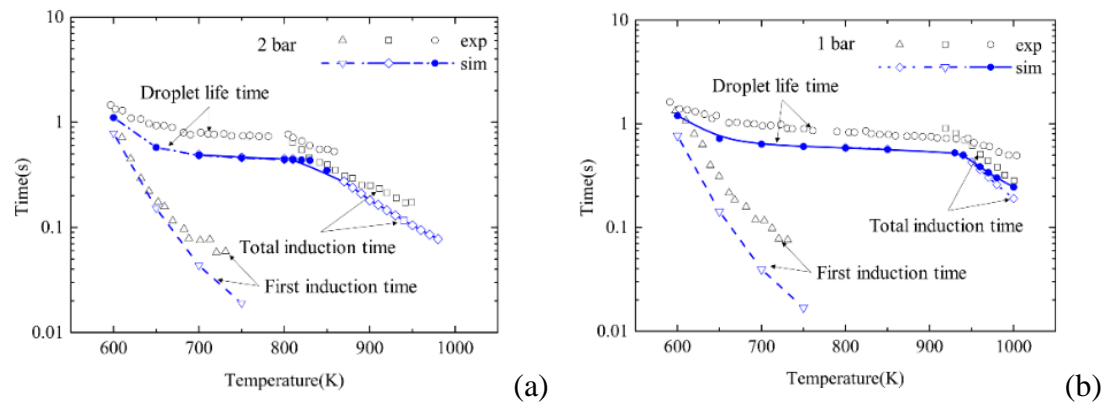


Figure 4.1 Droplet life time and induction times for n-heptane droplet: (a) 1 bar; (b) 2 bar.

The evolutions of maximum temperature and squared droplet sizes (D^2) from different conditions are shown in the left picture of Figure 4.2. For the cases of 1bar-600K, slow vaporization is followed by the ignition triggered after one half of the total droplet lifetime and the temperature stays around 800 K (cool flame) until the droplet is consumed. For 2bar-750K, due to much faster ignition, the droplet size evolution is vastly controlled by the low temperature oxidation, leading to a much shorter droplet lifetime. Single ignition is found for higher temperature, i.e. 1bar-980K, where the high temperature environments provides the base

for much faster vaporization even before the ignition. After ignition occurs, the high temperature oxidation pathway dominates and significantly accelerates the droplet vaporization. The right part of Fig. 4.2 shows how NC7KET24 accumulates and consumed to produce CH_2O and release heat in spatial coordinates. This spatially spreading feature indicates that the cool flame may be in a partially premixed combustion region.

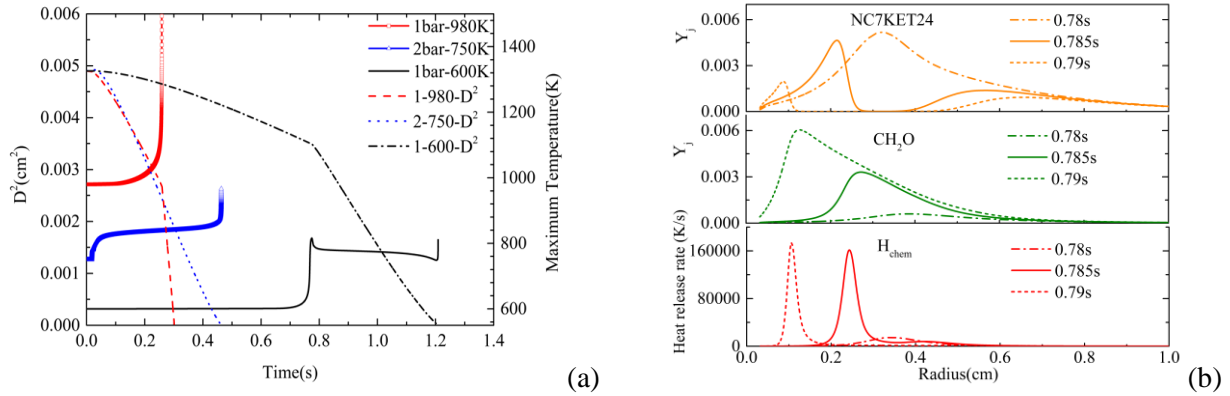


Figure 4.2 (a) The temperature and D^2 revolution of droplets under different initial conditions; (b) distribution of low temperature gateway species and heat that shows the ignition dynamic for the 1bar-600K case in (a).

Figure 4.3a shows the results for representative low pressure cases, i.e. 0.5 bar. The droplet lifetimes are found to be slightly longer than those in Fig. 4.2a. As the saturation pressure is only temperature dependent, lower pressure equilibrates the interface at a lower temperature so that the fuel concentration at the interface is limited by the resulting lower fuel concentration. Chemical-temporal oscillation after the “dumped cool flames” found in this study is consistent with Cuoci et al. (2015) [6]. Figure 4.3b displays the various burning types of droplets, the solid lines are the T-P conditions validated in prior studies that are bounded by our numerical results down to 0.1 bar (dashed lines for 0.1-1 bar). As we can see the two cool flame boundaries intersect at 0.1 bar and 600 K, the cool flame zone become a closed triangle. These data points in Figure 4.3b represent different burning states from the present study. The red points for hot single ignition; green for no ignition; blue for cool flame and yellow for two-stage ignition. Noticeable discrepancy between the points and these zones in the zone boundaries can be seen.

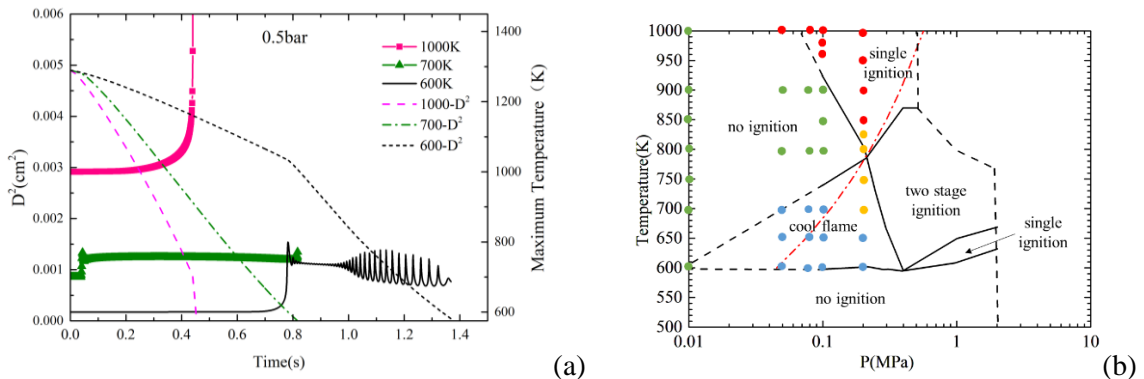


Figure 4.3 The T-P graph of various burning types of droplets in experiments and this simulation (points)

Shown in Figure 4.3b also is the ceiling temperature (the red dashed-dotted line) obtained from equilibrium calculation for gateway reaction pathways $\dot{\text{R}} + \text{O}_2 \leftrightarrow \text{ROO}$ for initiation of low temperature chemistry.

This pressure dependent curve is based on the Arrhenius parameters for oxygen molecule addition for C₇H₁₅-2 and C₇H₁₅-3 and corresponding peroxy decomposition reactions. The oxygen mole fraction is assumed to be 0.20. Through analyzing competitive pathways favoring alkyl radicals or peroxy radicals, or pyrolysis over oxidation [13], it should be found that the transition from the low temperature to high temperature mechanism occurs approximately at the ceiling temperature and is ruled by the decomposition of peroxy radicals. However, due to the transport processes, the red dashed-dotted line appears to be steeper than the boundary between cool flame and no ignition whereas this ceiling curve corresponds quite well with the boundary between hot single ignition and two-stage ignition. Noted that for some cases, low temperature oxidation dominates and brings the temperature across the ceiling curve. Therefore the two-stage zone plotted using initial temperature here is below the ceiling temperature. For droplets that started in the NTC temperature region, the increase of specific heat with temperature for major species reduces the temperature increase given the same heat release. This negative feedback effect leads to heat accumulation until the temperature reaches requirement for high temperature oxidation pathways where the increase of heat release becomes more competitive comparing to the increase of specific heat, hence causing the temperature jump for hot ignition. Unfortunately, not all the droplets survive before they acquire a high enough temperature for hot ignition. This is the key reason for those no ignition zones to appear above the ceiling curve. Steady cool flames are found to exist beyond this ceiling line, which needs further investigations.

5 Summary

Based on the results and analyses provided in the previous section, the following points summarize the present study:

- 1) The 1-D spherically symmetric modelling presented here provides well prediction to the experimental data for 1-2 bar.
- 2) Dynamic evolutions of species, maximum temperature, and heat release rate suggests the low temperature oxidation pathways do occur in an expected sequence
- 3) The effects of pressure dependent and critical chemical reactions as well as the interface equilibrium are bounded by the droplet lifetime and form an intrinsically rich regime diagram.
- 4) By using equilibrium calculations for the critical reaction pathway $\dot{R} + O_2 \leftrightarrow R\dot{O}O$, a pressure dependent ceiling temperature curve can be determined. While the two stage ignition brings the initial temperature across the ceiling, droplets initially in NTC regions need to survive long enough to turn no ignition into hot single ignition. This fundamental physics of droplet burning separates these two zones in the diagram. The discrepancy between cool flame boundary and the ceiling curve needs further investigations.

6 Acknowledgements

This project is supported by a seed grant for Space Mission Concept Development of National Space Science Center, Chinese Academy of Science and the Key Laboratory for Thermal Science and Power Engineering of Ministry of Education, Tsinghua University, Beijing, China. Discussions with ZhuYin Ren and Remy Mevel of Tsinghua Univ. regarding numerical methods and hydrocarbon oxidation pathways are very much appreciated.

References

- [1] Nayagam V, Haggard JB, Colantonio RO, Marchese AJ, Dryer FL, Zhang BL, Williams FA. (1998). Microgravity n-Heptane Droplet Combustion in Oxygen-Helium Mixtures at Atmospheric Pressure. *AIAA Journal*. 36(8): 1369.
- [2] Turns SR. (2011). *An Introduction to Combustion: Concepts and Applications*. McGraw-Hill Education. ISBN 0-073-38019-9.
- [3] Farouk TI, Dryer FL. (2014). Isolated n-heptane droplet combustion in microgravity: “Cool Flames”-Two-stage combustion. *Combustion and Flame*.161: 565.
- [4] Liu YC, Xu Y, Hicks M, Avedisian CT. (2016). Comprehensive study of initial diameter effects and other observations on convection-free droplet combustion in the standard atmosphere for n-heptane, n-octane, and n-decane. *Combustion and Flame*. 171: 27.
- [5] Tanabe M, Bolik T, Eigenbrod C, Rath HJ. (1996). Spontaneous ignition of liquid droplets from a view of nonhomogeneous mixture formation and transient chemical reactions. *Twenty-Sixth Symposium (International) on Combustion*. 1637.
- [6] Cuoci A, Frassoldati A, Faravelli T, Ranzi E. (2015). Numerical modeling of auto-ignition of isolated fuel droplets in microgravity. *Proceedings of the Combustion Institute*. 35: 1621.
- [7] Ji WQ, Zhao P, He TJ, He X, Farooq A, Law CK. (2015). On the controlling mechanism of the upper turnover states in the NTC regime. *Combustion and Flame*.164: 294.
- [8] Urzay J. (2018). Supersonic Combustion in Air-Breathing Propulsion Systems for Hypersonic Flight. *Annu. Rev. Fluid Mech*. 50: 593.
- [9] Farouk TI, Dryer FL. (2011). Microgravity droplet combustion: effect of tethering fiber on burning rate and flame structure. *Combustion Theory and Modelling*.15(4): 487.
- [10] Strang G. (1968). On the construction and comparison of difference schemes. *SIAM Journal on Numerical Analysis*. 5(3): 506.
- [11] Yoo CS, Lu T, Chen JH, Law CK. (2011). Direct numerical simulations of ignition of a lean n-heptane/air mixture with temperature inhomogeneities at constant volume: Parametric study. *Combustion and Flame*. 158: 1727.
- [12] Mehl M, Pitz WJ, Westbrook CK, Curran HJ. (2011). Kinetic modeling of gasoline surrogate components and mixtures under engine conditions. *Proceedings of the Combustion Institute*. 33: 193.
- [13] Bugler J, Somers KP, Silke EJ, Curran HJ. (2015). Revisiting the kinetics and thermodynamics of the low-temperature oxidation pathways of alkanes: A case study of the three pentane isomers. *J. Phys. Chem*. 119: 7510.